Intelligent MPPT system improved with sliding mode control

Said Dani, Asmaa Drighil, Khadija Abdouni, Khalid Sabhi
Laboratory of Information Processing, Department of Physics, Faculty of Sciences Ben M'Sick, University Hassan II,
Casablanca, Morocco

Article Info	ABSTRACT
	The sharp rise in global energy demand over recent decades has necessitated the exploration of alternative energy sources. Solar energy, known for being both pollution- and fuel-free, stands out as a preferred choice. However, its efficiency is sensitive to factors like temperature fluctuations and solar irradiation. To optimize energy extraction, a maximum power point tracking algorithm is crucial for photovoltaic systems. This paper proposes a robust sliding mode control enhanced with an artificial neural network to achieve the Maximum Power Point in a stand-alone PV system. The artificial neural network determines the reference voltage, which is then regulated by the sliding mode control to match the photovoltaic array voltage. The performance of the suggested controller is compared to that of a proportional-integral-based neural network controller and the perturb and observe method using MATLAB/Simulink. The results show that the suggested method provides excellent tracking performance and rapid convergence even under quickly changing weather conditions, highlighting its efficiency and robustness.

Corresponding Author:

Said Dani
Laboratory of Information Processing, Department of Physics, Faculty of Sciences Ben M'Sick
University Hassan II
Bd Driss ELHARTI BP 7955 Casablanca, Morocco
Email: said_dani@hotmail.fr

1. INTRODUCTION

The global energy demand has increased dramatically in recent decades, driven by rapid industrialization, urbanization, and population growth. This trend highlights the urgent need for sustainable energy solutions to replace fossil fuels, both finite and major contributors to environmental problems like climate change. Among renewable energy sources, solar energy is distinguished by its abundance and environmental benefits, and low maintenance requirements. Photovoltaic systems, in particular, provide clean, renewable energy and are particularly useful in remote areas.

However, daily and seasonal fluctuations in environmental factors, such as temperature and solar radiation, have a major impact on these systems. To address these challenges, maximum power point tracking (MPPT) techniques have been developed to optimize energy capture and enhance system performance under varying conditions [1]-[4].

In recent years, a variety of MPPT techniques have been proposed [5]-[8]. Traditional methods such as perturb and observe (P&O) [6] and incremental conductance (IC) [3] are widely renowned for their simplicity, low cost, and effectiveness under standard sunlight and temperature conditions. The perturb and observe (P&O) method is particularly preferred in areas with constant solar irradiation and minimal environmental variations. However, it faces significant challenges when dealing with rapidly changing conditions [7], including slower response times, persistent oscillations around the maximum power point, and

decreased tracking accuracy, which can limit their performance. These issues are especially critical in areas with rapidly changing weather conditions, such as tropical or mountainous regions [9].

Advanced MPPT methods, including fuzzy logic controllers (FLC), have been developed to address these challenges [10]-[14], genetic algorithms (GA) [15], [16]. When dealing with complex environmental variations, these techniques offer superior adaptability and efficiency. FLC-based approaches improve response times and mitigate oscillations [10], while GA proves highly effective in locating the global maximum power point, particularly under partial shading effects [17].

Artificial neural network-based algorithms have been widely studied in [18]-[21] for various applications. ANN-based MPPT systems that use RBFN architectures for non-linear PV arrays, integrate PI controllers for enhanced response time and stability, or use field-oriented control to optimize the frequency of the inverter can significantly improve the efficiency, stability, and reliability of photovoltaic systems [22]-[24]. Additionally, neural network approaches have been used in [25], [26] for applications such as PV pumping systems.

To further enhance performance, sliding mode controllers (SMCs) have been extensively proposed in the literature [17], [27]-[29]. These controllers ensure stable operation by maintaining a constant voltage at the load, even under varying environmental conditions, thus providing robustness and precision. A main contribution of this study is to improve the performance of maximum power point tracking (MPPT) by combining sliding mode control (SMC) with artificial neural networks (ANN). Although SMC usually suffers from chattering issues, this limitation has been overcome by using continuous functions. This results in smoother control signals, improving system stability and ensuring robust and efficient MPPT performance. Simulation results are used to evaluate the effectiveness of the suggested method, which is then compared to the standard P&O algorithm and the hybrid ANN-PI approach under diverse irradiance and temperature scenarios.

The paper is structured as follows: Section 2 deals with the modeling of the PV module and the DC-DC boost converter. Section 3 presents the architecture of the ANN and its role in generating the reference voltage. Section 4 describes the methodology used to design and implement the sliding-mode controller, highlighting how it reduces chattering and ensures system stability. Section 5 discusses the results in a comparative context, highlighting the advantages of the proposed method over traditional and hybrid approaches. Concluding the study, Section 6 proposes potential avenues for future research.

2.   SYSTEM MODELING
2.1. Photovoltaic model

Solar cells are semiconductor devices that generate direct current when sunlight hits their surface. The equivalent electrical circuit, known as the one-diode model, consists of a current source, a single diode, and two resistors, as shown in Figure 1 [23], [30]. The output current of a photovoltaic cell can be determined by applying the law of Kirchhoff, as shown in (1).

$$I_{pv} = I_{ph} - I_d - I_{sh} \ = I_{ph} - I_d \ - \frac{V_{pv} + I_{pv}.R_S}{R_{sh}} \tag{1}$$

According to the Shockley equation, the diode current I_d is given by (2).

$$I_d = I_0 \left(exp \left(\frac{q(V_{pv} + I_{pv}.R_S)}{nkT} \right) - 1 \right) \tag{2}$$

where I_0 represents the reverse saturation current, k represents the Boltzmann constant, q denotes the elementary charge, n signifies the ideality factor of the p-n junction, and T indicates the temperature of the photovoltaic cell [23]. The I-V characteristics of the PV cell model may be obtained by subsuming (2) into (1), as described by the formula below.

In (3) indicates how temperature T and irradiance I_r affect the photocurrent I_{ph}.

$$I_{pv} = I_{ph} - \left(exp \left(\frac{q(V_{pv} + I_{pv}.R_S)}{nkT} \right) - 1 \right) - \frac{V_{pv} + I_{pv}.R_S}{R_{sh}} \tag{3}$$

$$I_{ph} = [I_{sc} + k_i(T - 298).\frac{G}{1000} \tag{4}$$

Where G represents the solar irradiation, I_{sc} is the short circuit current at 25 °C and 1000 W/m², and k_i corresponds to the temperature coefficient of I_{sc}.

A photovoltaic module is generally composed of several PV cells arranged in series or parallel configurations. The photovoltaic module consists of n_P PV cells connected in parallel and n_s PV cells are

connected in series. Based on this configuration, the output voltage V and output current I of the module can be defined as (5) and (6).

$$V = n_s . V_{pv} \tag{5}$$

$$I = n_P . I_{pv} \tag{6}$$

We obtain the formula for the PV module's output current by substituting (5) and (6) into (3).

$$I = n_P . I_{ph} - n_P . I_0 \left(exp \left(\frac{q(\frac{V}{n_P} + \frac{I}{n_S} . R_S)}{nkT} \right) - 1 \right) - \frac{\frac{n_p}{n_S} . V + I . R_S}{R_{sh}} \tag{7}$$

The photovoltaic array described in this paper can generate a maximum output power of 100.8 kW under standard test conditions (STC). It consists of 64 strings, each containing 5 modules connected in series, with each module having a maximum power output of 315.073 W. The total power is calculated as follows: $64 \times 5 \times 315.072\,W = 100.8\,kW$. The parameters of the SunPower SPR-305E-WHT-D module under STC are presented in Table 1. The characteristics of the photovoltaic array, consisting of 5 series-connected modules and 64 parallel strings, are illustrated in Figures 2 and 3, showing the I-V and P-V curves under varying irradiance and temperature conditions, respectively.

Table 1. SunPower SPR-305E-WHT-D module parameters under STC

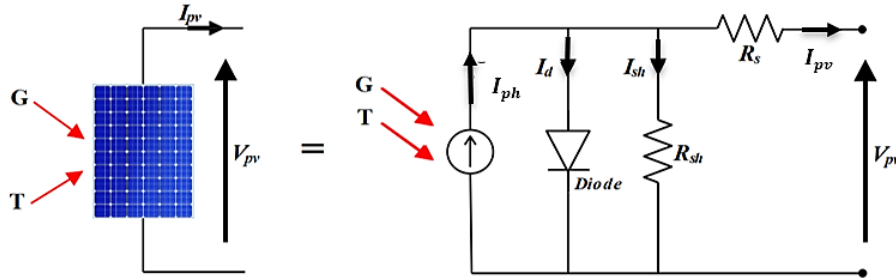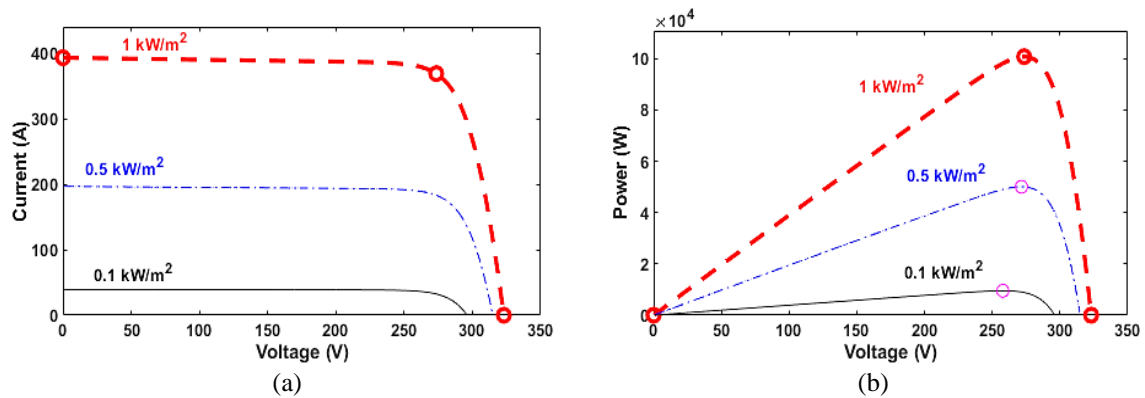| Parameter	Value
Maximum power P_{mpp}	315.073 W
Current at I_{mpp}	5.76 A
Voltage at V_{mpp}	54.7 V
Short-circuit current I_{sc}	6.14 A
Open-circuit voltage V_{oc}	64.6 V
No.of cells per module	96

Figure 1. Equivalent electrical circuit of photovoltaic cell

Figure 2. Comparison of the I-V and P-V characteristics of the PV array under varying irradiance levels at T = 25 °C in (a) I-V characteristic and (b) P-V characteristic

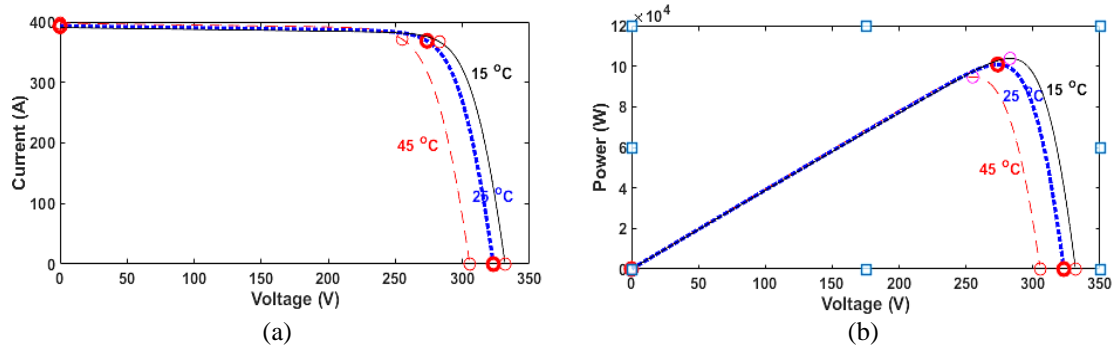Figure 3. Comparison of the I-V and P-V characteristics of the PV array under varying temperature
at G = 1000 W/m^2 in (a) I-V characteristic and (b) P-V characteristic

2.2. Boost converter modeling

The averaged model of the Boost converter is derived by applying the basic principles of system operation [31]. The converter diagram is shown in Figure 4. The dynamic equations for this converter are expressed as (8)-(10).

$$\begin{cases} \dot{x}_1 = \dfrac{i_{pv}}{C_1} - \dfrac{x_2}{C_1} & (8) \\[2mm] \dot{x}_2 = \dfrac{x_1}{L} - (1-u)\dfrac{x_3}{L} & (9) \\[2mm] \dot{x}_3 = -\dfrac{x_3}{RC_2} + (1-u)\dfrac{x_2}{C_2} & (10) \end{cases}$$

Where $x = [x_1\ x_2\ x_3] = [V_{PV}\ I_L\ V_0]$.

The boost converter, which is powered by the solar module, is subject to continuous input voltage variations due to changing weather conditions. Consequently, the duty cycle must be dynamically adjusted to ensure that the system tracks the maximum power point of the photovoltaic array. The electrical parameters of the boost converter are provided in Table 2.
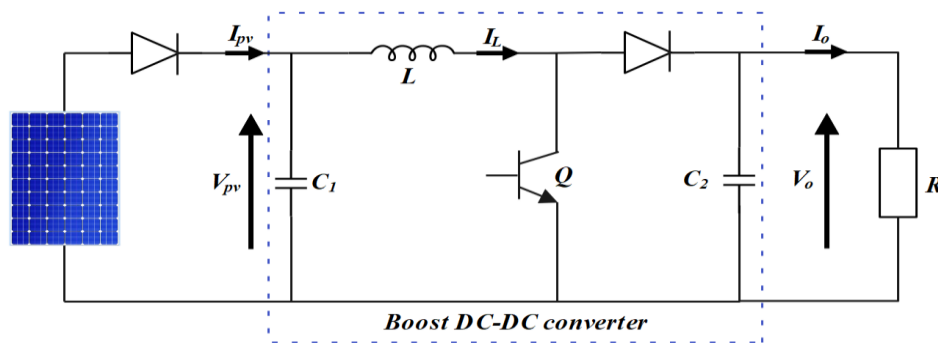

Figure 4. Boost converter schematic

Table 2. Main electrical parameters of the boost converter

Electrical parameter	Value
Inductor L	5 mH
Input capacitor C$_1$	1 mF
Output capacitor C$_2$	5 mF
Switching frequency f	5 KHz

3.   CONTROL OF THE SYSTEM

This paper presents a hybrid MPPT system combining ANN and SMC to enhance power extraction from photovoltaic (PV) systems, as shown in Figure 5. The ANN predicts the reference voltage (V_{ref}) at the maximum power point (MPP) by analyzing real-time solar irradiation and temperature variations. At the same time, the SMC calculates the duty cycle (u) by comparing V_{ref} with the actual PV voltage (V_{pv}). The duty cycle is then processed through pulse width modulation (PWM) to regulate the boost converter's switching (Q), ensuring that V_{pv} tracks V_{ref} and achieves MPP. The boost converter increases the PV panel voltage using an inductance (L_1), capacitors (C_1 and C_2), and diodes, coordinated through switching control. A resistive load was selected to simplify the experimental setup and facilitate the analysis of the system's core performance.
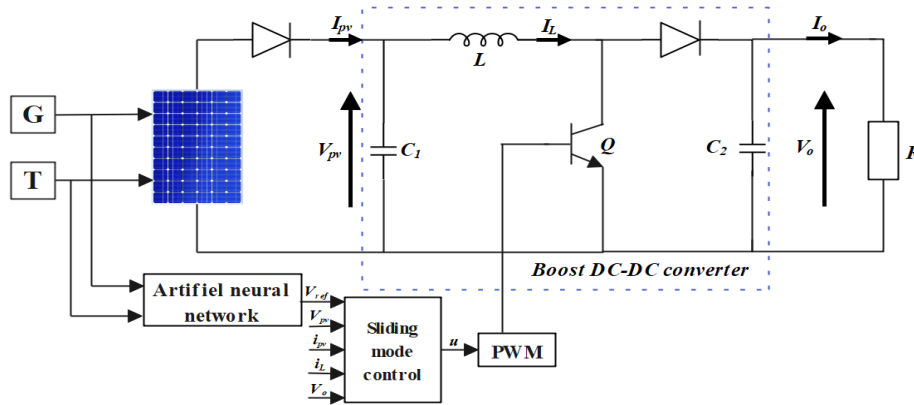

Figure 5. Proposed system

3.1. Generation of reference by neural networks MPP

The proposed ANN predicted the MPP voltage of the photovoltaic array. A feedforward neural network consisting of three layers has been implemented, as illustrated in Figure 6. The network receives temperature and solar irradiation as inputs, processes them through hidden layers, and outputs the reference voltage (V_{ref}) for the SMC.

a)   Input layer:

The input neurons receive the solar irradiation x_1 and temperature x_2. Each input neuron has a bias term, denoted as 1.

b)   Hidden layer

The net input to a hidden neuron i is given by:

$$z_i = \sum_{j=1}^{2} w_{ij}\, x_j + b_i \tag{11}$$

Where x_j are the input signals (solar irradiation x_1 and temperature x_2); w_{ij} are the weights from the input neurons j to the hidden neuron i; and b_i is the bias term for the hidden neuron i. The output of the hidden neuron i after applying the activation function (sigmoid function σ) is (12).

$$h_i = \sigma(z_i) = \frac{1}{1+e^{-z_i}} \tag{12}$$

c)   Output layer:

The net input to the output neuron k is given by (13).

$$z_k = \sum_{i=1}^{n} w_{ki}\, h_i + b_k \tag{13}$$

Where h_i are the outputs from the hidden neurons; w_{ki} are the weights from the hidden neurons i to the output neuron k; b_k is the bias term for the output neuron k; and the output of the network, which is the V_{ref} voltage value at the MPP is (14).

$$y_k = z_k = V_{ref} \tag{14}$$

The database for this study, derived from photovoltaic module simulations, includes irradiation patterns, temperature variations, and the corresponding MPP voltage, as illustrated in Figure 7. This dataset is divided as follows: 70% is used for training, 15% for validation, and 15% for testing the feedforward neural network. To train the neural network effectively for predicting the target variable, the mean square error (MSE) serves as the loss function, as indicated in (9). The MSE assesses the accuracy of the network's predictions by averaging the squared differences between the predicted and actual values. Through gradient-based optimization, this error is minimized by iteratively adjusting the model's parameters, thereby improving its predictive performance over time.

Figure 8 shows the performance of the ANN, showing an MSE of 3.6775e^{-02}, which indicates satisfactory results.

$$MSE = \frac{1}{n} \sum_{i=1}^{n} (V_{ref}(i) - \hat{V}_{ref}(i))^2 \tag{15}$$

Where n is the number of data points; $V_{ref}(i)$ is the actual voltage for the *i-th* data point; and $\hat{V}_{ref}(i)$ is the predicted voltage for the *i-th* data point.
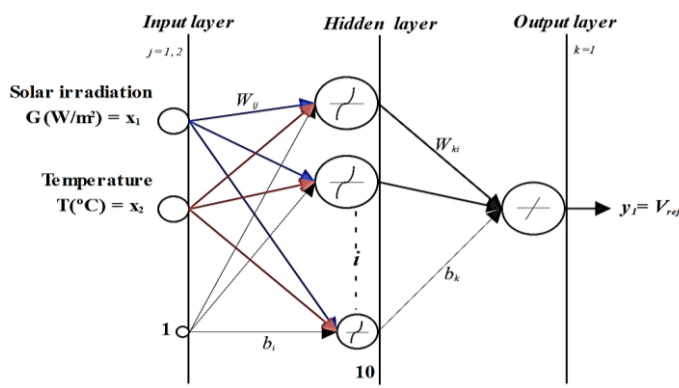

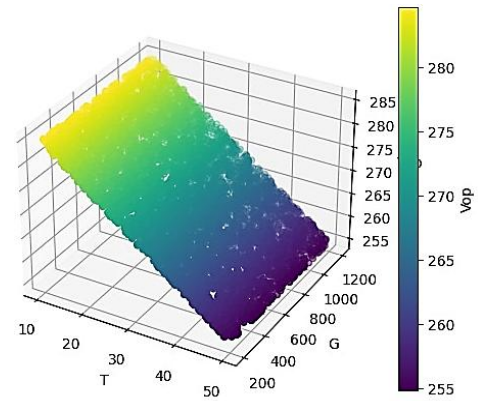Figure 6. The proposed ANN architecture

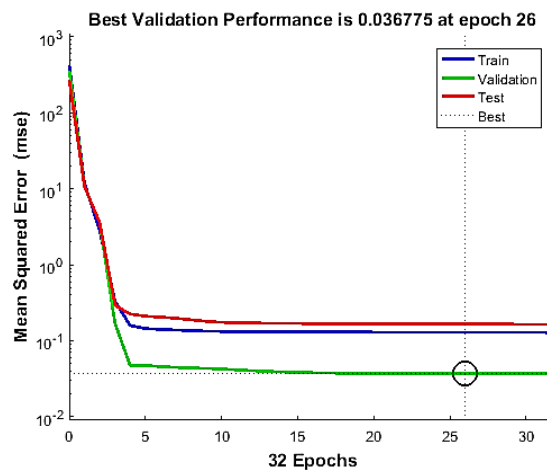Figure 7. The optimal PV voltage according to the environmental conditions

Figure 8. Mean square error

3.2. Sliding mode control design

Sliding mode control (SMC) is a nonlinear technique that has been developed for use with highly nonlinear systems, such as photovoltaic arrays. The fundamental objective of the SMC is to offer stability and optimal energy transfer between the PV array and the DC load. The SMC method involves defining a sliding surface and designing a control law that maintains the system state at this surface. By continuously adjusting

the control input, this method ensures that the system remains at the MPP of the photovoltaic array, effectively adapting to varying weather conditions [31].

This section presents the SMC design using a reference voltage, $x_{1d} = V_{ref}$ when feeding the ANN. The sliding surface of this control is defined as (16).

$$e_1 = x_1 - x_{1d} \tag{16}$$

Where $x_{1d} = V_{ref}$. Taking the derivative of (16) along the dynamics given in (2).

$$\dot{e}_1 = \dot{x}_1 - \dot{x}_{1d}$$
$$\dot{e}_1 = \frac{i_{pv}}{C_1} - \frac{x_2}{C_1} - \dot{x}_{1d} \tag{17}$$

The second error,

$$e_2 = \dot{e}_1 \tag{18}$$

Taking the derivative of e_2,

$$\dot{e}_2 = \ddot{e}_1 = \frac{1}{C_1} \cdot \frac{di_{pv}}{dt} - \frac{\dot{x}_2}{C_1} - \ddot{x}_{1d}$$
$$\dot{e}_2 = \frac{1}{C_1} \cdot \frac{di_{pv}}{dt} - \frac{x_1}{LC_1} + \frac{x_3}{LC} - \frac{x_3}{LC_1} \cdot u - \ddot{x}_{1d} \tag{19}$$

The sliding surface S is defined as (20).

$$S = e_2 + \alpha. e_1 \tag{20}$$

The derivative of (14).

$$\dot{s} = \ddot{e}_1 + \alpha \dot{e}_1 = \dot{e}_2 + \alpha \dot{e}_1 \tag{21}$$

Substituting in (17) and (19) into (21),

$$\dot{s} = \frac{i_{pv}}{C_1} - \frac{x_1}{LC_1} + \frac{x_3}{LC_1} - \frac{x_3}{LC_1} \cdot u - \ddot{x}_{1d} + \alpha \frac{i_{pv}}{C_1} - \alpha \frac{x_2}{C_1} - \alpha \dot{x}_{1d}$$

Setting $\dot{s} = 0$ gives the equivalent control law, denoted by u_{eq}, which is crucial for achieving the desired tracking, i.e $x_1 - x_{1d} = 0$.

$$\frac{i_{pv}}{C_1} - \frac{x_1}{LC_1} + \frac{x_3}{LC_1} - \frac{x_3}{LC_1} \cdot u_{eq} - \ddot{x}_{1d} + \alpha \frac{i_{pv}}{C_1} - \alpha \frac{x_2}{C_1} - \alpha \dot{x}_{1d} = 0$$
$$u_{eq} = \frac{LC_1 x_3}{x_3} \left[\frac{i_{pv}}{C_1} - \frac{x_1}{LC_1} + \frac{x_3}{LC_1} - \ddot{x}_{1d} + \alpha \frac{i_{pv}}{C_1} - \alpha \frac{x_2}{C_1} - \alpha \dot{x}_{1d} \right] \tag{22}$$

The reaching law is defined as follows: $u_s = +K. sign(S)$ with $K > 0$. The total control law for the nonlinear SMC-based MPPT system can be described as (23).

$$u = u_{eq} + u_s \tag{23}$$

SMC is robust and effective in handling nonlinearity, but often suffers from chattering due to the discontinuous switching term $u_s = +K. sign(S)$, which leads to high frequencies. To address this, the suggested method replaces the sign function with a continuous saturation function, represented as: $u_s = +K. sat(S/\emptyset)$. Where $\emptyset$ defines a boundary layer around the sliding surface. This adjustment smoothens the control input, reducing oscillations while maintaining accuracy.

Stability analysis uses the Lyapunov stability function, which is defined as (24).

$$V = \frac{1}{2} S^2$$
$$\dot{V} = S \left[\frac{i_{pv}}{C_1} - \frac{x_1}{LC_1} + \frac{x_3}{LC_1} - \frac{x_3}{LC_1} \cdot u - \ddot{x}_{1d} + \alpha \left(\frac{i_{pv}}{C_1} - \frac{x_2}{C_1} - \dot{x}_{1d} \right) \right] \tag{24}$$

Substituting (17) in (18).

$$\dot{V} = S\left[\frac{i_{pv}}{C_1} - \frac{x_1}{LC_1} + \frac{x_3}{LC_1} - \frac{x_3}{LC_1} \cdot \left(u_{eq} + K.sat(S/\emptyset)\right) - \ddot{x}_{1d} + \alpha\left(\frac{i_{pv}}{C_1} - \frac{x_2}{C_1} - \dot{x}_{1d}\right)\right]$$

$$\dot{V} = S.\left(-\frac{x_3}{LC_1}\right).K.sat\left(\frac{S}{\emptyset}\right)$$

The saturation function $sat(S/\emptyset)$ is bounded by $-1 \le sat(S/\emptyset) \le 1$. Therefore:

$$\dot{V} = -\left\|\frac{x_3}{LC_1}\right\|.K.|S|.\frac{|S|}{\emptyset} < 0$$

This indicates that the Lyapunov function V decreases as time passes, confirming the stability of the system while mitigating chattering due to the use of the continuous saturation function.

4.   RESULTS AND DISCUSSION

In order to assess the effectiveness, the proposed MPPT method, a simulation model was developed using MATLAB/Simulink. Figure 9 shows the simulation model of the photovoltaic system with the ANN-SMC MPPT technique. Specifically, Figure 9(a) represents the complete system architecture, and Figure 9(b) details the implementation of the SMC algorithm. The performance of the ANN-SMC controller was evaluated under various weather condition scenarios, as shown in Figure 10.
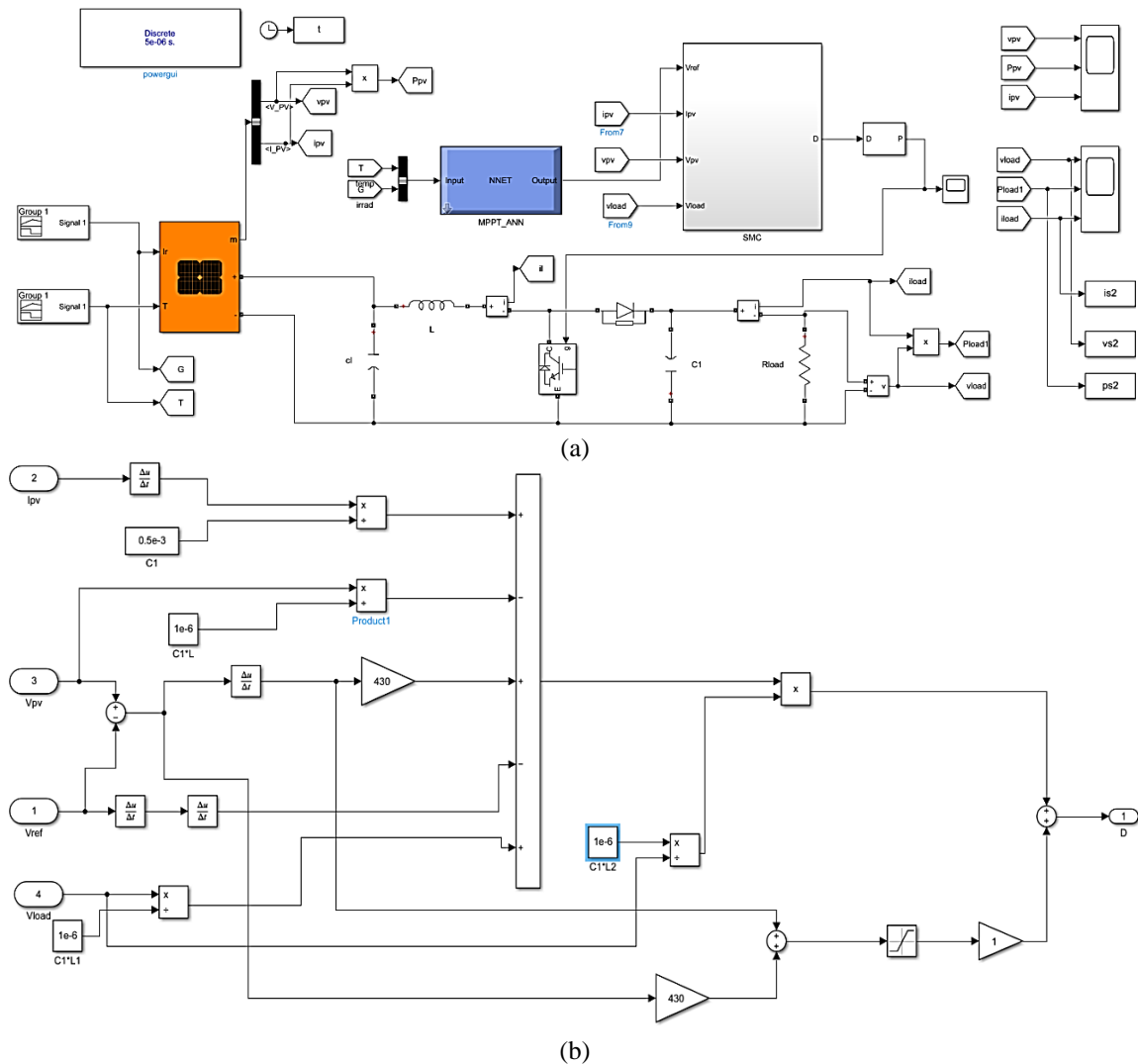

(a)

(b)

Figure 9. Simulation model of the photovoltaic system with ANN-SMC MPPT in Simulink:
(a) overall system architecture in Simulink and (b) detailed implementation of the SMC

To evaluate its adaptability, the system was tested in three different operating scenarios. During the first time interval (0 to 0.5 s), the photovoltaic module functioned under STC, with an irradiance of 1000 W/m² and a temperature of 25 °C. In the second time interval (0.5 s to 1 s), the irradiance was decreased from 1000 W/m² to 500 W/m², and the temperature was decreased from 25 °C to 15 °C. In the final time interval (1 s to 1.5 s), the irradiance was increased from 500 W/m² to 800 W/m², while the temperature was maintained at a constant 30 °C, to evaluate the system's response under improved solar conditions.

The MATLAB/Simulink simulation model includes a photovoltaic (PV) array, which is modeled using a single-diode equivalent circuit, a boost converter to regulate the voltage V_{pv}, and an MPPT controller that implements the ANN-SMC approach. The ANN-SMC controller integrates an ANN to estimate the reference voltage (V_{ref}) and an SMC to ensure robust tracking of V_{ref}. The ANN is trained on a dataset covering different irradiance and temperature variations, enabling it to dynamically predict the optimal value. The SMC uses a sliding surface designed to minimize tracking error while mitigating chattering effects.

To evaluate the efficiency of the ANN-SMC controller, a comparative analysis was conducted against two reference MPPT techniques: perturb and observe (P&O) and ANN-PI. As illustrated in Figure 11, the power output response demonstrates the superior performance of ANN-SMC, which rapidly reaches the MPP with minimal oscillations. In contrast, P&O exhibits slower convergence and higher oscillations, while ANN-PI achieves better results than P&O but remains less stable than ANN-SMC. The improved stability of ANN-SMC is further confirmed by the voltage and current responses shown in Figures 12 and 13. ANN-SMC ensures smoother voltage and current transitions with minimal fluctuations compared to the other methods, while P&O suffers from excessive oscillations and ANN-PI faces moderate instability.
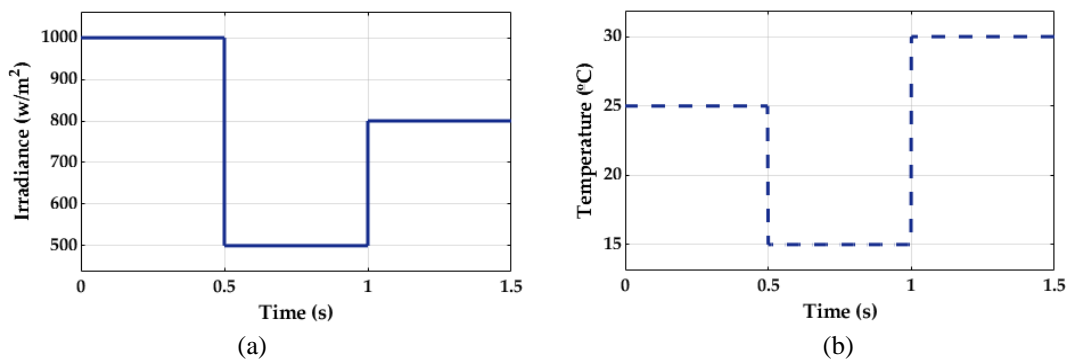

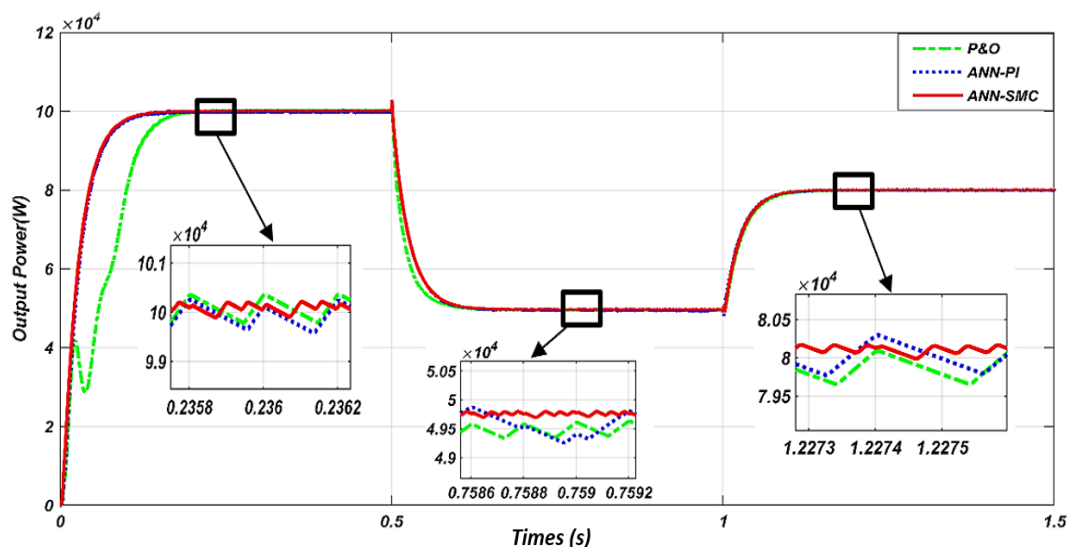Figure 10. Weather conditions: (a) irradiance and (b) temperature

Figure 11. Power output generated by ANN-SMC, ANN-PI, and P&O methods
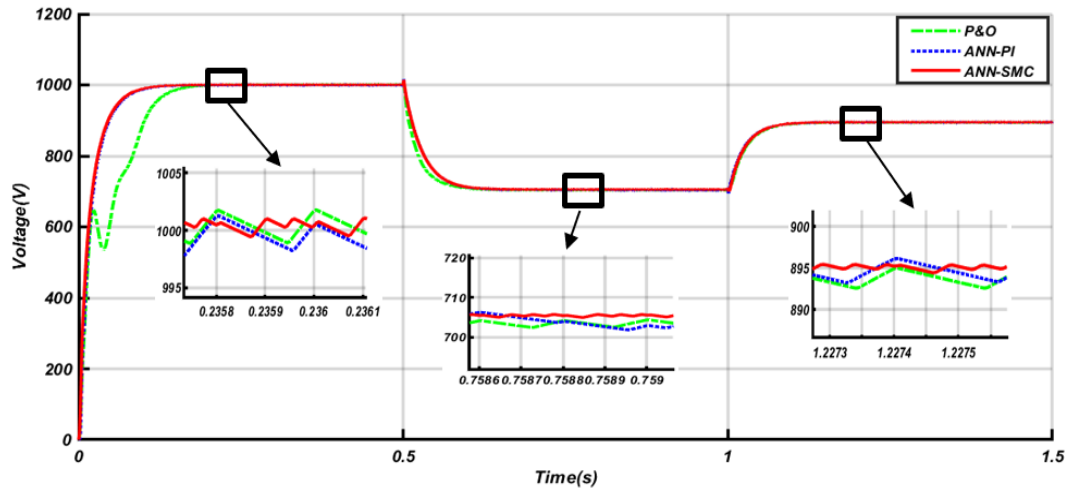under diverse weather conditions

Figure 12. Voltage output generated by ANN-SMC, ANN-PI, and P&O methods
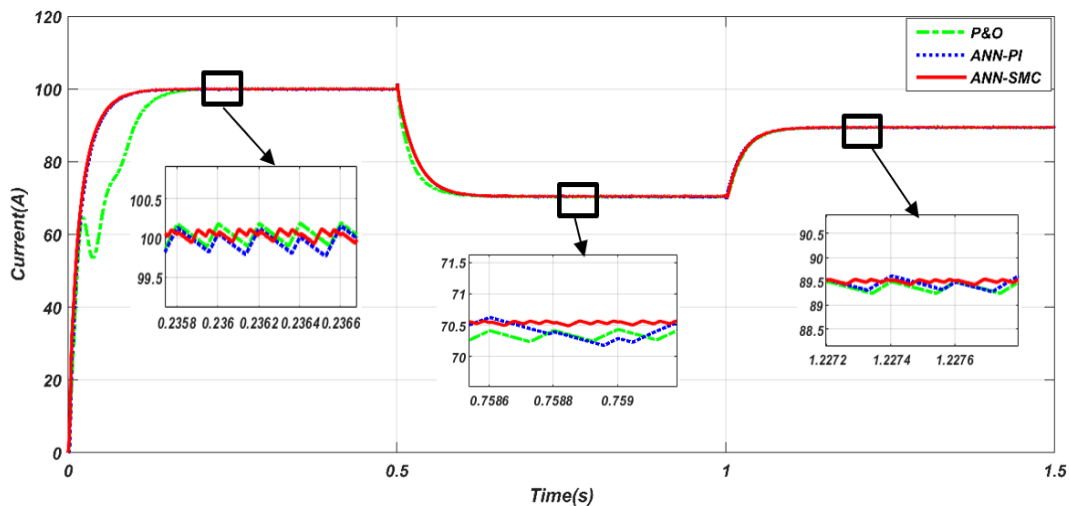under diverse weather conditions

Figure 13. Current output generated by ANN-SMC, ANN-PI, and P&O methods
under diverse weather conditions

Table 3 shows clear advantages of the ANN-SMC method over P&O and ANN-PI in tracking the MPP for MPPT algorithms. The ANN-SMC technique demonstrates superior accuracy, rapid adaptability to changing environmental conditions, and exceptional stability across different climates. The results clearly show the strengths of ANN-SMC over ANN-PI and P&O techniques, positioning it as a highly effective solution for enhancing the MPPT performance of solar photovoltaic systems.

Table 3. Comparison results of ANN-SMC, ANN-PI, and P&O methods

	Temperature 25 ℃ Irradiance 1000 W/m²		Temperature 15 ℃ Irradiance 500 W/m²		Temperature 30 ℃ Irradiance 800 W/m²	
MPPT method	Power oscillation (kW)	Tracking response time (s)	Power oscillation (kW)	Tracking response time (s)	Power oscillation (kW)	Tracking response time (s)
ANN-SMC	0.1	0.12	0.1	0.55	0.08	1.15
ANN-PI	0.3	0.14	0.2	0.60	0.15	1.2
P&O	0.6	0.25	0.4	0.65	0.3	1.25

5. CONCLUSION

This study demonstrates the effectiveness of the ANN-SMC technique for maximum power point tracking (MPPT) in PV systems, highlighting its clear advantages over ANN-PI and P&O methods in terms of

accuracy, responsiveness, and reliability under variable conditions. The use of a continuous saturation function significantly reduces the chattering effect, making the approach both energy efficient and stable.

While the use of resistive loads helps simplify the analysis, it limits the realism of the evaluation. Future research will focus on evaluating how the system performs with non-linear loads and grid integration to confirm its practical applicability in real photovoltaic systems. In addition, efforts could focus on improving the computational efficiency and extending the method to other renewable energy applications. Furthermore, as the proposed approach has been tested using simulations, future work will consider an experimental implementation to determine its real-world feasibility and ensure its robustness under practical operating conditions.

FUNDING INFORMATION

AUTHOR CONTRIBUTIONS STATEMENT
This journal uses the Contributor Roles Taxonomy (CRediT) to recognize individual author contributions, reduce authorship disputes, and facilitate collaboration.

Name of Author	C	M	So	Va	Fo	I	R	D	O	E	Vi	Su	P	Fu
Said Dani	✓	✓	✓	✓	✓	✓	✓	✓	✓	✓	✓			
Asmaa Drighil	✓	✓			✓					✓		✓	✓	
Khadija Abdouni				✓	✓			✓		✓				
Khalid Sabhi					✓		✓			✓				

C : **C**onceptualization	I : **I**nvestigation	Vi : **Vi**sualization
M : **M**ethodology	R : **R**esources	Su : **Su**pervision
So : **So**ftware	D : **D**ata Curation	P : **P**roject administration
Va : **Va**lidation	O : Writing - **O**riginal Draft	Fu : **Fu**nding acquisition
Fo : **Fo**rmal analysis	E : Writing - Review & **E**diting	

CONFLICT OF INTEREST STATEMENT
Authors state no conflict of interest.

DATA AVAILABILITY
The data that support the findings of this study are available from the corresponding author, [SD], upon reasonable request.

REFERENCES
[1]   Y. Liu, X. Liu, J. Zhang, Y. Zhang, and Z. Zhu, "A novel maximum power point tracking control strategy for the building integrated photovoltaic system," *Energies*, vol. 13, no. 11, p. 2679, May 2020, doi: 10.3390/en13112679.
[2]   H. Liu, M. Y. A. Khan, and X. Yuan, "Hybrid maximum power extraction methods for photovoltaic systems: a comprehensive review," *Energies*, vol. 16, no. 15, p. 5665, Jul. 2023, doi: 10.3390/en16155665.
[3]   P. K. Mishra and P. Tiwari, "Incremental conductance MPPT in grid connected PV system," *International Journal of Engineering, Science and Technology*, vol. 13, no. 1, pp. 138-145, 2021, doi: 10.4314/ijest.v13i1.21S.
[4]   E. Mendez-Flores, A. Ortiz, I. Macias, and A. Molina, "Experimental validation of an enhanced MPPT algorithm and an optimal DC–DC converter design powered by metaheuristic optimization for PV systems," *Energies*, vol. 15, no. 21, p. 8043, Oct. 2022, doi: 10.3390/en15218043.
[5]   M. L. Katche, A. B. Makokha, S. O. Zachary, and M. S. Adaramola, "A comprehensive review of maximum power point tracking (MPPT) techniques used in solar PV systems," *Energies*, vol. 16, no. 5, p. 2206, Feb. 2023, doi: 10.3390/en16052206.
[6]   M. H. Ibrahim, S. P. Ang, M. N. Dani, M. I. Rahman, R. Petra, and S. M. Sulthan, "Optimizing step-size of perturb & observe and incremental conductance MPPT techniques using PSO for grid-tied PV system," *IEEE Access*, vol. 11, pp. 13079–13090, 2023, doi: 10.1109/ACCESS.2023.3242979.
[7]   R. Singh and P. Basak, "Modelling and simulation of a PV generator and MPPT using P&O method and fuzzy logic controller," *International Journal of Advanced Research in Electrical, Electronics and Instrumentation Engineering*, vol. 04, no. 07, pp. 5827–5835, Jul. 2015, doi: 10.15662/ijareeie.2015.0407004.
[8]   H. H. Ammar, A. T. Azar, R. Shalaby, and M. I. Mahmoud, "Metaheuristic optimization of fractional order incremental conductance (FO-INC) Maximum power point tracking (MPPT)," *Complexity*, vol. 2019, no. 1, Jan. 2019, doi: 10.1155/2019/7687891.

[9]   F. L. Tofoli, D. De Castro Pereira, et W. J. De Paula, "Comparative study of maximum power point tracking techniques for photovoltaic systems," *International Journal of Photoenergy*, vol. 2015, p. 1-10, 2015, doi: 10.1155/2015/812582.

[10] J.-K. Shiau, Y.-C. Wei, et B.-C. Chen, "A study on the fuzzy-logic-based solar power MPPT algorithms using different fuzzy input variables," *Algorithms*, vol. 8, no. 2, p. 100-127, avr. 2015, doi: 10.3390/a8020100.

[11] M. Alshareef, "An improved MPPT method based on fuzzy logic controller for a PV system," *STUD INFORM CONTROL*, vol. 30, no 1, p. 89-98, 2021, doi: 10.24846/v30i1y202108.

[12] D. Remoaldo et I. Jesus, "Analysis of a Traditional and a fuzzy logic enhanced perturb and observe algorithm for the MPPT of a photovoltaic system," *Algorithms*, vol. 14, no. 1, p. 24, 2021, doi: 10.3390/a14010024.

[13] S. Chowdhury, D. Kumar Das, and M. S. Hossain, "Power performance evaluation of a PV module using MPPT with fuzzy logic control," *Journal of Engineering Advancements*, vol. 2, no. 01, pp. 07–12, Jan. 2021, doi: 10.38032/jea.2021.01.002.

[14] U. Yilmaz, A. Kircay, et S. Borekci, "PV system fuzzy logic MPPT method and PI control as a charge controller," *Renewable and Sustainable Energy Reviews*, vol. 81, p. 994-1001, 2018, doi: 10.1016/j.rser.2017.08.048.

[15] S. Hadji, J.-P. Gaubert, and F. Krim, "Experimental analysis of genetic algorithms based MPPT for PV systems," in *2014 International Renewable and Sustainable Energy Conference (IRSEC)*, IEEE, Oct. 2014, pp. 7–12. doi: 10.1109/IRSEC.2014.7059887.

[16] E. S. Wirateruna, M. J. Afroni, and A. F. Ayu, "Implementation of PSO algorithm on MPPT PV System using Arduino Uno under PSC," *International Journal of Artificial Intelligence & Robotics (IJAIR)*, vol. 5, no. 1, pp. 13–20, May 2023, doi: 10.25139/ijair.v5i1.6029.

[17] A. Hassan, O. Bass, et M. A. S. Masoum, « An improved genetic algorithm based fractional open circuit voltage MPPT for solar PV systems », *Energy Reports*, vol. 9, p. 1535-1548, déc. 2023, doi: 10.1016/j.egyr.2022.12.088.

[18] M. S. Karabinaoğlu, B. Çakır, M. E. Başoğlu, A. Kazdaloğlu, and A. Günereoğlu, "Comparison of deep learning and regression-based MPPT algorithms in PV systems," *Turkish Journal of Electrical Engineering and Computer Sciences*, vol. 30, no. 6, pp. 2319–2338, Sep. 2022, doi: 10.55730/1300-0632.3941.

[19] K. Abdouni, H. Ennasri, A. Drighil, H. Bahri, M. Bour, and M. Benboukous, "Efficient and robust nonlinear control MPPT based on artificial neural network for PV system," *International Journal of Power Electronics and Drive Systems (IJPEDS)*, vol. 15, no. 3, p. 1914, Sep. 2024, doi: 10.11591/ijpeds.v15.i3.pp1914-1924.

[20] Asif, W. Ahmad, M. B. Qureshi, M. M. Khan, M. A. B. Fayyaz, and R. Nawaz, "Optimizing large-scale PV systems with machine learning: a neuro-fuzzy MPPT control for PSCs with uncertainties," *Electronics*, vol. 12, no. 7, p. 1720, Apr. 2023, doi: 10.3390/electronics12071720.

[21] K. Sabhi, M. Talea, and H. Bahri, "Improving power precision in hybrid renewable energy systems with a quad active bridge DC-DC converter and neural network-based decoupling," in *2024 International Conference on Intelligent Systems and Computer Vision (ISCV)*, IEEE, May 2024, pp. 1–8. doi: 10.1109/ISCV60512.2024.10620155.

[22] S. E. Eyimaya, "Efficiency analysis of artificial intelligence and conventional maximum power point tracking methods in photovoltaic systems," *Applied Sciences*, vol. 15, no. 10, p. 5586, May 2025, doi: 10.3390/app15105586.

[23] M. Yilmaz and M. Corapsiz, "Artificial neural network based MPPT algorithm with boost converter topology for stand-alone PV system," *Erzincan Üniversitesi Fen Bilimleri Enstitüsü Dergisi*, vol. 15, no. 1, pp. 242–257, Mar. 2022, doi: 10.18185/erzifbed.1002823.

[24] M. Yilmaz, R. Celikel, and A. Gundogdu, "Enhanced photovoltaic systems performance: anti-windup pi controller in ANN-based ARV MPPT method," *IEEE Access*, vol. 11, pp. 90498–90509, 2023, doi: 10.1109/ACCESS.2023.3290316.

[25] H. Dakhil Atiya, M. Boukattaya, and F. Ben Salem, "Integration of Fuzzy logic and neural networks for enhanced MPPT in PV systems under partial shading conditions," *Iraqi Journal for Electrical and Electronic Engineering*, vol. 21, no. 1, pp. 1–15, Jun. 2025, doi: 10.37917/ijeee.21.1.1.

[26] A. Hmidet *et al.*, "Design of efficient off-grid solar photovoltaic water pumping system based on improved fractional open circuit voltage MPPT technique," *International Journal of Photoenergy*, vol. 2021, pp. 1–18, Oct. 2021, doi: 10.1155/2021/4925433.

[27] Y. Zhang, Y.-J. Wang, and J.-Q. Yu, "A novel MPPT algorithm for photovoltaic systems based on improved sliding mode control," *Electronics*, vol. 11, no. 15, p. 2421, Aug. 2022, doi: 10.3390/electronics11152421.

[28] I. U. Haq *et al.*, "Neural network-based adaptive global sliding mode MPPT controller design for stand-alone photovoltaic systems," *PLOS ONE*, vol. 17, no. 1, p. e0260480, Jan. 2022, doi: 10.1371/journal.pone.0260480.

[29] B. Deffaf, F. Hamoudi, N. Debdouche, Y. A. Amor, and S. Medjmadj, "Super-twisting sliding mode control for a multifunctional double stage grid-connected photovoltaic system," *Advances in Electrical and Electronic Engineering*, vol. 20, no. 3, Oct. 2022, doi: 10.15598/aeee.v20i3.4454.

[30] S. Jenkal *et al.*, "Development of a photovoltaic characteristics generator based on mathematical models for four PV panel technologies," *International Journal of Electrical and Computer Engineering (IJECE)*, vol. 10, no. 6, p. 6101, Dec. 2020, doi: 10.11591/ijece.v10i6.pp6101-6110.

[31] H. Y. Ahmed, O. Abdel-Rahim, and Z. M. Ali, "New high-gain transformerless DC/DC boost converter system," *Electronics*, vol. 11, no. 5, p. 734, Feb. 2022, doi: 10.3390/electronics11050734.

BIOGRAPHIES OF AUTHORS
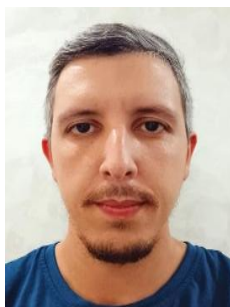
Said Dani 🆔 🈁 SC ⟳ was born in Casablanca, Morocco, in 1990. He received his master's degree in Information Processing at the University Hassan II, Faculty of Science Ben M'Sick, in 2023. He earned his Ph.D. in the application of artificial intelligence techniques to track the maximum operating point of a photovoltaic system at the Information Processing Laboratory at the University Hassan II of Casablanca. He can be contacted at email: said_dani@hotmail.fr.

Asmaa Drighil 🆔 �"> SC ◔ was born in Morocco in 1970. She received a master's in Solid State Physics, Matter and Radiation, at the Faculty of Science Ben M'Sick, from the University Hassan II, in Casablanca, Morocco, in 1997. In 2000, she received her Ph.D. in 'Characterization of defects in semi-insulators (CdTe and CdZnTe) and solar photocells (GaAs and Si)' in the laboratory of Engineering and Materials, Faculty of Sciences, Ben M'Sick, from University Hassan II. She is currently a Professor in the Physics Department at the Faculty of Science Ben M'Scik, University Hassan II, Casablanca, Morocco. Her research in the information processing laboratory consists of renewable energy. She can be contacted at email: doc.drighil@gmail.com.

Khadija Abdouni 🆔 �"> SC ◔ was born in Casablanca, Morocco, in 1998. She received her master's degree in Information Processing at the University Hassan II, Faculty of Science Ben M'sick, in 2019. She earned her Ph.D. in the application of artificial intelligence techniques to track the maximum operating point of a photovoltaic system at the Information Processing Laboratory at the University Hassan II of Casablanca. She can be contacted at email: abdounikhadija8@gmail.com.

Khalid Sabhi 🆔 �"> SC ◔ was born in Morocco in 1990. He is a Ph.D. student at the Laboratory of Information Processing, FSBM Casablanca, Hassan 2 University in Morocco. In 2014, he graduated with honors from Morocco's Faculty of Science and Technology of FES with a degree in Mechatronic Engineering. His research activities include the design, control, and intelligent management of renewable hybrid energy systems. He can be contacted at email: sabhi.khalid.imt@gmail.com.